

## Aerosol-Assisted Formation of Mesostructured Thin Films\*\*

By Yunfeng Lu,\* Byron F. McCaughey, Donghai Wang,  
J. Eric Hampsey, Nilesh Doke, Zhengzhong Yang,  
and C. Jeffrey Brinker\*

Surfactant-templated mesoporous materials have attracted much attention due to their unique structures and potential applications.<sup>[1–3]</sup> Synthesis of these materials involves the formation of surfactant–inorganic nanocomposites via co-assembly of surfactant and inorganic species and subsequent surfactant removal to create mesoporous materials with controlled pore structures (e.g., hexagonal or cubic arrangement of pores or lamellar nanostructures<sup>[1,3–5]</sup>) and with various macroscopic forms (e.g., powders,<sup>[1–3,6]</sup> particles,<sup>[7–10]</sup> thin films,<sup>[8,11–16]</sup> and fibers<sup>[17,18]</sup>). Mesoporous thin films are of particular interest because of their potential applications as sensors, membranes, and low dielectric constant films.<sup>[13,19,20]</sup> Synthesis methods include solution deposition<sup>[12,21]</sup> and solvent evaporation-induced self-assembly (EISA).<sup>[8,13,15,16,22]</sup> In the solution deposition method, thin films spontaneously nucleate and grow from acidic aqueous silicate solutions containing high concentrations of surfactant. This slow deposition process (time scale of hours to days) usually results in hexagonally ordered granular thin films with pore channels oriented parallel to the substrate surface. The EISA route deposits thin films using a rapid dip- or spin-coating process (time scale of seconds), during which solvent evaporation enriches the concentration of silicate and surfactant, inducing their co-assembly into mesostructured, defect-free surfactant–silicate thin films.<sup>[13,23]</sup>

This research describes a novel approach that combines aerosol deposition<sup>[24–26]</sup> and EISA to fabricate mesostructured

thin films. As shown in Figure 1, this method starts with an acidic precursor solution containing a silica source and surfactant. Solvent evaporation from the aerosol droplets enriches them in silicate and surfactant and induces their co-assembly into semi-solid mesostructured particles.<sup>[8]</sup> These semi-solid particles then further coalesce on the substrate resulting in a continuous mesostructured thin film with no evidence of its original particle morphology. Compared with the dip-coating or spin-coating processes, this method can rapidly deposit mesostructured thin films with easily controlled mesostructures on large-scale planar and non-planar substrates.

Figure 1 shows the scheme of the aerosol deposition apparatus. The atomizer (TSI Model # 3076) was operated under laminar flow conditions using 2.6 L min<sup>-1</sup> of N<sub>2</sub> as the carrier/atomization gas. The heating zone was maintained at 150 °C or less. The residence times for the entrained aerosol particles in the drying and heating zones are approximately 3 s each. Introduction of HCl vapor into the reactor was conducted using a coaxial tube positioned at the center of the heating zone. Thin films were deposited on silicon substrates or holey carbon transmission electron microscope (TEM) grids for a period of seconds to minutes in the manner shown in Figure 1. The thickness of the deposited thin films (up to several micrometers) is controlled by the deposition time.

Representative TEM images shown in Figure 2 for a series of B56, P123, and F127 surfactant-templated thin films demonstrate that the mesostructure is tunable depending on the templating surfactant utilized. The mesostructured thin film in Figure 2A was templated with B56 surfactant, deposited on a silicon substrate, and calcined at 400 °C for 1 h in air to remove the surfactant. This calcined B56 thin film exhibits a highly ordered cubic mesostructure with a unit cell parameter of 64 Å ( $d_{100} = 64$  Å), which is similar to those of dip-coated or spin-coated thin films.<sup>[27]</sup> Note that one-dimensional shrinkage upon calcination may distort the thin film mesostructure and result in a “brick-like” structure as shown in Figure 2A.<sup>[13,28]</sup> Such ultra-thin (~400 Å thick) mesostructured thin films with three-dimensional pore channels should exhibit a low transport resistance and thus are useful for membrane and separation applications. Figure 2B,C show TEM images of an uncalcined thin film deposited using P123 surfactant. They indicate a continuous hexagonal mesostructure oriented parallel to the substrate with a unit parameter of around 98 Å. The swirling pattern of the tube bundles (Fig. 2C) shows no preferred orientation in plane, which is consistent with the low bending energy of the tubules and the inability of the liquid–vapor interface to impose long-range order on the tubule assembly process.<sup>[12,13]</sup> A TEM plan-view image (Fig. 2D) of a thin film prepared using F127 surfactant demonstrates the formation of a continuous, ordered, mesostructured thin film with a unit cell parameter of around 170 Å.

Figure 3 shows the XRD patterns of calcined B56-templated and uncalcined P123-templated thin films deposited on a silicon wafer. The B56-templated thin film exhibits a sharp cubic (200) reflection at 32 Å, consistent with the TEM result shown in Figure 2A. The P123-templated thin film shows an

[\*] Prof. Y. Lu, B. F. McCaughey, D. Wang, J. E. Hampsey  
Department of Chemical Engineering, Tulane University  
New Orleans, LA 70118 (USA)  
E-mail: ylu@tulane.edu

Prof. C. J. Brinker, N. Doke  
Sandia National Laboratories and  
Department of Chemical and Nuclear Engineering  
The University of New Mexico  
Albuquerque, NM 87131 (USA)  
E-mail: cjbrink@sandia.gov

Prof. Z. Yang  
State Key Laboratory of Polymer Physics and Chemistry  
Center for Molecular Science, Institute of Chemistry  
The Chinese Academy of Sciences  
Beijing 100080 (China)

[\*\*] This work was partially supported by the Louisiana Board of Regents under the grant number LEQSF (2001-04)-RD-B-09, by NASA under the grant NAG-1-02070 and NCC-3-946, by the Advanced Materials Research Institute at the University of New Orleans through DARPA Grant No. MDA972-97-1-0003, and through the Louisiana Board of Regents Contract No. NSF/LEQSF(2001-04)-R-II-03. This work was also partially supported by the U.S. National Science Foundation NIRT program Grant Number EEC-0210835, the U.S. Department of Energy (DOE) Basic Energy Sciences Program and Sandia National Laboratory's Laboratory Directed R&D program. Sandia is a multiprogram laboratory operated by Sandia Corporation, a Lockheed Martin Company, for DOE under contract DE-AC04-94 ALB5000.

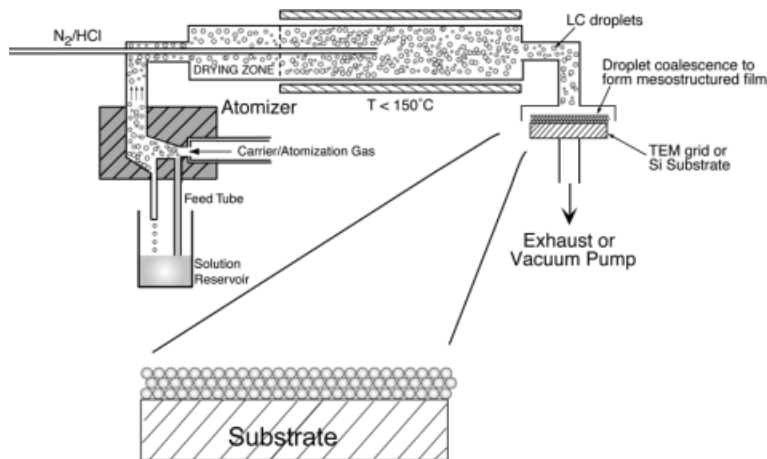


Fig. 1. Schematic illustration of the aerosol apparatus used for thin film deposition.

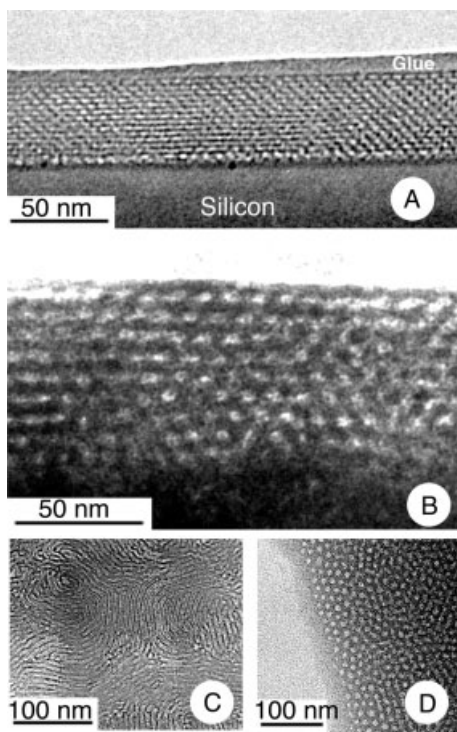


Fig. 2. TEM images of the aerosol-deposited mesostructured thin films. A) Cross-section image of a calcined B56-templated thin film; B) cross-section and C) plan-view images of an uncalcined P123-templated thin film; D) plan-view image of a F127-templated thin film.

intense hexagonal (100) reflection at 98 Å along with higher order (200) and (300) reflections. Note the absence of (110) and (210) reflections due to pore channel orientation parallel to the substrate surface.<sup>[28]</sup> Calcination of the P123-templated thin film results in a similar XRD pattern but with the (100) reflection at a lower *d*-spacing (70 Å). Combination of the TEM and XRD results indicates that mesostructured thin films can be readily prepared using surfactant self-assembly in combination with the aerosol deposition technique.

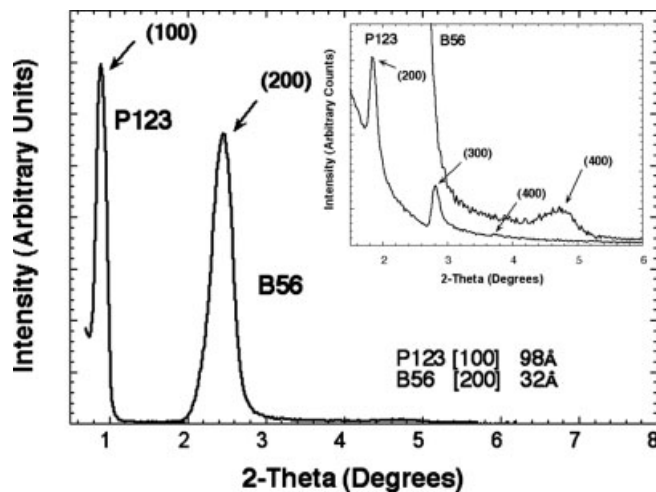


Fig. 3. X-ray diffraction of the aerosol thin films deposited on silicon wafers using B56 and P123 surfactants.

A possible formation mechanism for these thin films involves the coalescence and subsequent mesostructural transformation of the semisolid surfactant–silica nanocomposite particles on a substrate, causing a transition from spherical particles to planar thin films. During the aerosol process, the EISA of silica and surfactant results in the formation of semi-solid spherical particles containing lamellar, cubic, or hexagonal mesostructures. Since the degree of silica condensation is low,<sup>[29]</sup> these semi-solid particles may coalesce into a thin film to decrease their curvature and to minimize surface energy upon their deposition on a flat substrate surface. The transformation from a spherical to a planar morphology results in meso-scale structural reassembly within the thin films. According to this proposed mechanism, an increased degree of silica condensation should promote particle solidification and inhibit coalescence and mesostructure reassembly.

We examined this hypothesis by increasing the heating zone temperature or by introducing HCl vapor to promote silica condensation reactions.<sup>[29]</sup> Plan-view TEM images in Figure 4

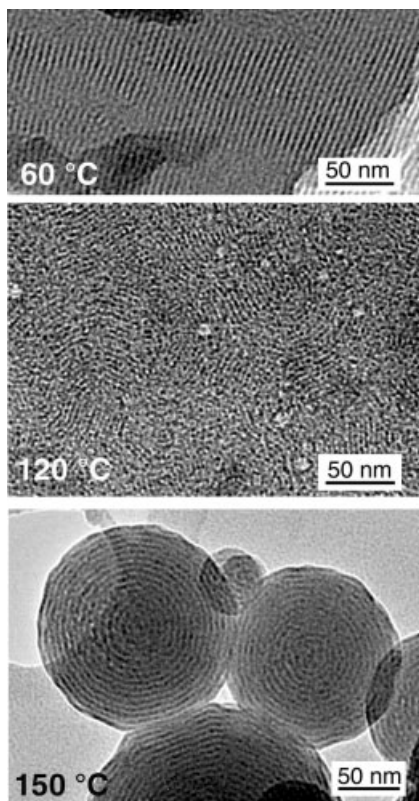


Fig. 4. TEM images of the thin films deposited on TEM grids using B56 surfactant at 60, 120, and 150 °C.

and XRD scans in Figure 5 of the silica–B56 thin films deposited using 60, 120 and 150 °C heating zone temperatures demonstrate that an increase in temperature decreases the degree of ordering. Figure 4 clearly indicates that an increase in the deposition temperature results in a change in the thin film morphology from a continuous long-range ordered mesostructure, to a continuous short-range ordered mesostructure, and finally to partly coalesced particles with an ordered vesicular structure similar to previously reported results.<sup>[8]</sup> XRD of the film deposited on silicon wafers at 60 °C (see Fig. 5) shows an intense narrow peak accompanied by a second order peak, suggesting that the film contains highly ordered mesostructures. With an increase of deposition temperature, the diffraction peaks become weaker and wider with the absence of the second order peak, showing that the degree of mesostructure order decreases. These results clearly indicate that a relatively low heating zone temperature creates a more ordered thin film because a less condensed silica network promotes coalescence of the particles, reassembly of the mesostructure, and formation of a continuous mesostructured thin film.

Figure 6 shows a TEM image of the mesostructured silica–P123 particles exposed to HCl vapor during their deposition onto a TEM grid. It clearly shows partially coalesced particles composed of a well-evolved and stiffened silicate mesostructure. Although the deposition process is conducted at room temperature, the HCl vapor catalyzes silica condensation reactions, ‘freezing’ the coalescence and reassembly process at

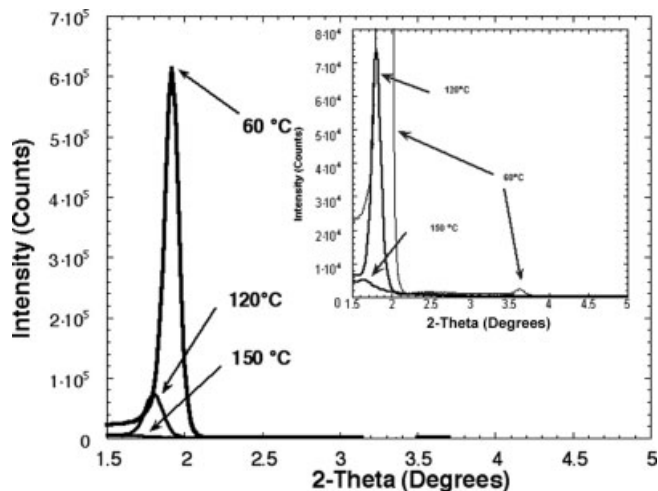


Fig. 5. X-ray diffraction of the aerosol thin films deposited on silicon wafer using B56 and P123 surfactants at 60, 120, and 150 °C.

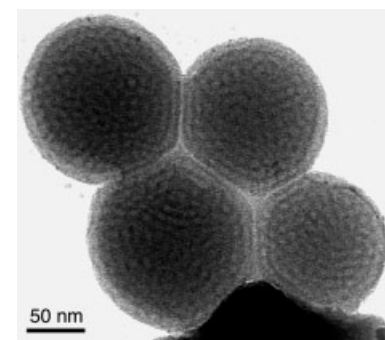


Fig. 6. TEM images of coalescing silica–P123 mesostructured particles with evolving mesostructures frozen by the HCl vapor.

an intermediate stage. Comparison of the particulate hexagonal mesostructure shown in Figure 6 and those shown in Figures 2B,C clearly suggests that the mesostructures of the deposited thin films are developed by mesostructure reassembly. These temperature change and HCl experiments strongly support the mechanism proposed above and indicate that a relatively low degree of silica condensation reaction favors particle coalescence, mesostructure reassembly, and the formation of a continuous mesostructured thin film.

We have developed a new approach towards mesostructured thin films using combined surfactant self-assembly and aerosol deposition techniques. The formation mechanism involves solvent evaporation-induced self-assembly of aerosol droplets with subsequent mesostructure reassembly and particle coalescence on a substrate. A lower degree of silica condensation favors particle coalescence, mesostructure reassembly, and the formation of continuous mesostructured thin films. A higher degree of silica condensation inhibits this reassembly and results in the formation of particles or mesostructured thin films with a less ordered mesostructure. These techniques are simple and can potentially be used to prepare ultra-thin or large-area mesostructured films on various substrates.

Experimental

Precursor solutions were prepared by mixing 1.25 g of surfactant, 1.2 mL of 0.07 M HCl, 0.6 mL of water, 20 mL of ethanol, and 10 mL of stock solution. The stock solution was prepared by refluxing tetraethoxysilane (TEOS, Si(OCH<sub>2</sub>CH<sub>3</sub>)<sub>4</sub>), ethanol, water, and dilute HCl (molar ratio: 1:3.8:1.5 × 10<sup>-5</sup>) at 60 °C for 90 min [27]. The surfactants used were Brij-56 (B56, CH<sub>3</sub>(CH<sub>2</sub>)<sub>15</sub>-(OCH<sub>2</sub>CH<sub>2</sub>)<sub>10</sub>-OH), Pluronic-P123, (P123, (EO)<sub>20</sub>(PO)<sub>70</sub>(EO)<sub>20</sub>), and Pluronic-F127, (F127, (EO)<sub>105</sub>(PO)<sub>70</sub>(EO)<sub>105</sub>), where EO is ethylene oxide and PO is propylene oxide. Calcination of the thin films conducted at 400 °C in air for 3 h using a heating rate of 1 °C min<sup>-1</sup> resulted in homogenous crack-free thin films. The mesostructure was characterized using TEM (JEOL 2010 apparatus) operated at 200 KV and a Siemens D500 X-ray diffractometer (XRD) with Ni-filtered CuKα radiation at λ = 1.5418 Å.

Received: April 30, 2003  
Final version: June 27, 2003

[1] J. Beck, J. Vartuli, W. Roth, M. Leonowicz, C. Kresge, K. Schmitt, C. Chu, D. Olson, S. Ew, S. McCullen, *J. Am. Chem. Soc.* **1992**, *114*, 10834.  
[2] C. Kresge, M. Leonowicz, W. Roth, C. Vartuli, J. Beck, *Nature* **1992**, *359*, 710.  
[3] G. A. Ozin, E. Chomski, D. Khushalani, M. J. MacLachlan, *Curr. Opin. Colloid Interface Sci.* **1998**, *3*, 181.  
[4] Q. Huo, D. I. Margolese, U. Clesla, P. Feng, T. E. Gler, P. Slegler, R. Leon, P. M. Petroff, F. Schuth, G. D. Stucky, *Science* **1994**, *368*, 317.  
[5] S. Burkett, S. Sims, S. Mann, *Chem. Commun.* **1996**, 1367.  
[6] J. S. Beck, J. C. V. Vartuli, *Curr. Opin. Solid State Mater. Sci.* **1996**, *1*, 76.  
[7] Q. Huo, J. Feng, F. Schuth, G. D. Stucky, *Chem. Mater.* **1997**, *9*, 14.  
[8] Y. Lu, H. Fan, A. Stump, T. L. Ward, T. Reiker, C. J. Brinker, *Nature* **1999**, *398*, 223.  
[9] S. Schacht, Q. Huo, I. G. Voigt-Martin, G. D. Stucky, F. Schuth, *Science* **1996**, *273*, 768.  
[10] H. Yang, G. Vovk, N. Coombs, I. Sokolov, G. A. Ozin, *J. Mater. Chem.* **1998**, *8*, 743.  
[11] H. Yang, N. Coombs, I. Sokolov, G. Ozin, *Nature* **1996**, *381*, 589.  
[12] I. Aksay, M. Trau, S. Manne, I. Honma, N. Yao, L. Zhou, P. Fenter, R. Eisenberger, S. Gruner, *Science* **1996**, *273*, 892.  
[13] Y. Lu, R. Ganguli, C. Drewien, M. Anderson, C. J. Brinker, W. Gong, Y. Guo, H. Soyoz, B. Dunn, M. Huang, J. Zink, *Nature* **1997**, *389*, 364.  
[14] A. Sellinger, P. M. Weiss, A. Nguyen, Y. Lu, R. A. Assink, W. Gong, C. J. Brinker, *Nature* **1998**, *394*, 256.  
[15] M. Ogawa, *J. Am. Chem. Soc.* **1994**, *116*, 7941.  
[16] M. Ogawa, *Chem. Commun.* **1996**, 1149.  
[17] P. J. Bruinsma, A. Y. Kim, J. Liu, S. Baskaran, *Chem. Mater.* **1997**, *9*, 2507.  
[18] P. Yang, D. Zhao, B. F. Chmelka, G. D. Stucky, *Chem. Mater.* **1998**, *10*, 2033.  
[19] Y. Lu, L. Hang, C. J. Brinker, T. M. Niemczyk, G. P. Lopez, *Sens. Actuators, B* **1996**, *35*, 1.  
[20] C. J. Brinker, M. T. Andeson, Y. Lu, R. Ganguli, *US Patent 5 858 457*, **1999**.  
[21] H. Yang, N. Coombs, O. Dag, I. Sokolov, G. Ozin, *J. Mater. Chem.* **1997**, *7*, 1755.  
[22] C. J. Brinker, Y. Lu, A. Sellinger, H. Fan, *Adv. Mater.* **1999**, *11*, 579.  
[23] C. J. Brinker, A. Hurd, P. Schunk, G. Frye, C. Ashley, *J. Non-Cryst. Solids* **1992**, *147/148*, 424.  
[24] J. D. Jorden, R. A. Dunbar, D. J. Hook, H.-Z. Zhuang, J. A. Gardella, L. A. Colon, F. V. Bright, *Chem. Mater.* **1998**, *10*, 1041.  
[25] J. D. Jorden, R. A. Dunbar, F. V. Bright, *Anal. Chim. Acta* **1996**, *83*, 332.  
[26] P. Marage, M. Langlet, J. C. Joubret, *Thin Solid Films* **1994**, *218*, 238.  
[27] D. Zhao, Q. Huo, J. L. Feng, B. F. Chmelka, G. D. Stucky, *J. Am. Chem. Soc.* **1998**, *120*, 6024.  
[28] H. Yang, A. Kuperman, N. Coombs, S. Mamiche-Afara, G. Ozin, *Nature* **1996**, *379*, 703.  
[29] C. J. Brinker, G. W. Scherer, *Sol-gel science: the physics and chemistry of sol-gel processing*, Academic Press, San Diego, CA **1990**.

Anisotropy in the Mobility and Photogeneration of Charge Carriers in Thin Films of Discotic Hexabenzocoronenes, Columnarly Self-Assembled on Friction-Deposited Poly(tetrafluoroethylene)\*\*

By Jorge Piris, Michael G. Debije, Natalie Stutzmann, Anick M. van de Craats, Mark D. Watson, Klaus Müllen, and John M. Warman\*

One of the main driving forces behind the intense study of discotic liquid crystalline materials since their discovery more than a quarter of a century ago,<sup>[1]</sup> has been their potential application in molecular electroluminescent, photovoltaic, and field-effect transistor devices. Harnessing their unique properties of columnar selforganization, selfhealing, and one-dimensional (1D) conduction has, however, proven elusive. A considerable advance in this direction was the finding by Zimmermann et al.<sup>[2]</sup> that uniaxial orientation of a mesomorphic derivative of triphenylene could be achieved by spin-coating onto a friction-deposited layer of poly(tetrafluoroethylene) (PTFE). More recently, van de Craats and co-workers<sup>[3,4]</sup> have shown that an oriented PTFE layer can induce the macroscopic columnar alignment of mesomorphic hexabenzocoronene derivatives (HBCs) by surface self-assembly from solution. Uniaxial columnar alignment over several square centimeters, even in the absence of a primer layer, has also recently been achieved by zone-casting directly onto a glass substrate.<sup>[5]</sup> In this work, we show that the mobility of charge carriers in PTFE-aligned HBC films is highly anisotropic with transport along the columns favored by more than an order of magnitude. Interestingly, the optical absorption and photogeneration efficiency of mobile charge carriers can display either a large or almost no anisotropy, depending on whether the aromatic cores of the columns are oriented perpendicular to or are tilted by close to 45° with respect to the columnar axis. In the former case, optical absorption is favored for light polarized perpendicular to the preferred direction of charge

\*] Dr. J. M. Warman, J. Piris, Dr. M. G. Debije  
Radiation Chemistry Department, IRI  
Delft University of Technology  
Mekelweg 15, NL-2629 JB Delft (The Netherlands)  
E-mail: warman@iri.tudelft.nl

Dr. N. Stutzman,<sup>[+]</sup> Dr. A. M. van de Craats<sup>[++]</sup>  
Cavendish Laboratory, University of Cambridge  
Madingley Road, Cambridge CB3 0HE (UK)

Dr. M. D. Watson, Prof. K. Müllen  
Max-Planck-Institut für Polymerforschung  
Ackermannweg 10, D-55128 Mainz (Germany)

[+] Present address: Philips Research, Prof. Holstlaan 4, NL-5656 AA Eindhoven, The Netherlands.

[++] Present address: Nederlands Forensisch Instituut (NFI), Volmerlaan 17, NL-2288 GD Rijswijk, The Netherlands.

\*\*] This research was carried out within the EU Framework 5 project "DIS-CEL" (Nr. G5RD-CT-2000-00321). N. S. expresses her gratitude to the Swiss National Science Foundation for financial support based on a Young Researcher Grant.